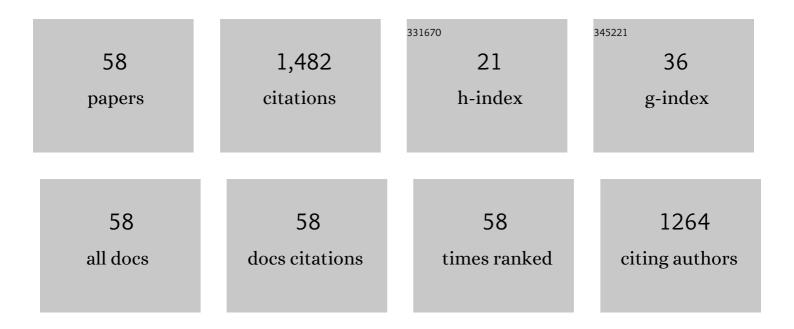
List of Publications by Year in descending order

Source: https://exaly.com/author-pdf/2900367/publications.pdf Version: 2024-02-01



#	Article	IF	CITATIONS
1	A review on fundmental research of oxy-coal combustion technology. Thermal Science, 2022, 26, 1945-1958.	1.1	4
2	Efficient CO2 reduction with H2O via photothermal chemical reaction based on Au-MgO dual catalytic site on TiO2. Journal of CO2 Utilization, 2022, 55, 101801.	6.8	9
3	Photothermal Chemistry Based on Solar Energy: From Synergistic Effects to Practical Applications. Advanced Science, 2022, 9, e2103926.	11.2	61
4	Elaborated Reaction Pathway of Photothermal Catalytic CO <sub>2</sub> Conversion with H <sub>2</sub> O on Gallium Oxideâ€Decorated and â€Defective Surfaces. Chemistry - A European Journal, 2022, , .	3.3	1
5	Photothermal Catalytic Water Splitting at Diverse Two-Phase Interfaces Based on Cu–TiO <sub>2</sub> . ACS Applied Energy Materials, 2022, 5, 4564-4576.	5.1	12
6	Introduction and preliminary testing of a 5Âm3/h hydrogen production facility by Iodine–Sulfur thermochemical process. International Journal of Hydrogen Energy, 2022, 47, 25117-25129.	7.1	11
7	Enhanced defect-water hydrogen evolution method for efficient solar utilization: Photo-thermal chemical coupling on oxygen vacancy. Chemical Engineering Journal, 2021, 408, 127248.	12.7	12
8	Photothermal Catalysis for Selective CO <sub>2</sub> Reduction on the Modified Anatase TiO <sub>2</sub> (101) Surface. ACS Applied Energy Materials, 2021, 4, 7702-7709.	5.1	21
9	Theoretical Study of Oxygen Vacancy on Indium Oxide for Promoted Photothermal Catalytic Water Splitting. Journal of Physical Chemistry C, 2021, 125, 19294-19300.	3.1	4
10	Accelerating photoelectric CO2 conversion with a photothermal wavelength-dependent plasmonic local field. Applied Catalysis B: Environmental, 2021, 298, 120533.	20.2	17
11	Thermal decomposition and combustion characteristics of Al/AP/HTPB propellant. Journal of Thermal Analysis and Calorimetry, 2021, 143, 3935-3944.	3.6	30
12	High-Performance Pt Catalyst with Graphene/Carbon Black as a Hybrid Support for SO <sub>2</sub> Electrocatalytic Oxidation. Langmuir, 2020, 36, 20-27.	3.5	13
13	The Influence of Anionic Additives on the Microwave Dehydration Process of Lignite. Energy & Fuels, 2020, 34, 9401-9410.	5.1	11
14	Standalone Solar Carbon-Based Fuel Production Based on Semiconductors. Cell Reports Physical Science, 2020, 1, 100101.	5.6	18
15	Visible light-responding perovskite oxide catalysts for photo-thermochemical CO2 reduction. Catalysis Communications, 2020, 138, 105955.	3.3	21
16	Pathway Alteration of Water Splitting via Oxygen Vacancy Formation on Anatase Titanium Dioxide in Photothermal Catalysis. Journal of Physical Chemistry C, 2020, 124, 26214-26221.	3.1	19
17	United Conversion Process Coupling CO <sub>2</sub> Mineralization with Thermochemical Hydrogen Production. Environmental Science & Technology, 2019, 53, 12091-12100.	10.0	3
18	Effects of Nafion content in membrane electrode assembly on electrochemical Bunsen reaction in high electrolyte acidity. International Journal of Hydrogen Energy, 2019, 44, 11646-11654.	7.1	9

#	Article	IF	CITATIONS
19	H2SO4 poisoning of Ru-based and Ni-based catalysts for HI decomposition in Sulfur Iodine cycle for hydrogen production. International Journal of Hydrogen Energy, 2019, 44, 9771-9778.	7.1	6
20	Influence of catalyst coated membranes on electrochemical bunsen reaction in the sulfur-iodine cycle. International Journal of Hydrogen Energy, 2019, 44, 9735-9742.	7.1	7
21	Enhanced Solar Conversion of CO <sub>2</sub> to CO Using Mnâ€doped TiO <sub>2</sub> Based on Photoâ€thermochemical Cycle. ChemistrySelect, 2019, 4, 236-244.	1.5	7
22	Catalyst Screening and Development for HI Decomposition in Sulfur-iodine Thermochemical Cycle for Hydrogen Production. Chemistry Letters, 2018, 47, 700-703.	1.3	2
23	Effect of iodine precipitation on HI separation subsection in sulfur-iodine cycle for hydrogen production. International Journal of Hydrogen Energy, 2018, 43, 10896-10904.	7.1	9
24	Photothermal Coupling Factor Achieving CO <sub>2</sub> Reduction Based on Palladium-Nanoparticle-Loaded TiO <sub>2</sub> . ACS Catalysis, 2018, 8, 6582-6593.	11.2	124
25	SO3 decomposition over CuO–CeO2 based catalysts in the sulfur–iodine cycle for hydrogen production. International Journal of Hydrogen Energy, 2018, 43, 14876-14884.	7.1	15
26	Catalytic performance of semi-coke on hydrogen iodide decomposition in sulfur-iodine thermochemical cycle for carbon dioxide-free hydrogen production. Energy Conversion and Management, 2018, 173, 659-664.	9.2	13
27	Effect of hydrothermal dewatering on the pyrolysis characteristics of Chinese low-rank coals. Applied Thermal Engineering, 2018, 141, 70-78.	6.0	48
28	Study of the mechanism of the catalytic decomposition of hydrogen iodide (HI) over carbon materials for hydrogen production. International Journal of Hydrogen Energy, 2017, 42, 4977-4986.	7.1	7
29	Pyrolysis Characteristics and Evolution of Char Structure during Pulverized Coal Pyrolysis in Drop Tube Furnace: Influence of Temperature. Energy & Fuels, 2017, 31, 4799-4807.	5.1	40
30	Exergy of Blackbody Radiation and Monochromatic Photon. International Journal of Thermophysics, 2017, 38, 1.	2.1	17
31	Guiding effective nanostructure design for photo-thermochemical CO2 conversion: From DFT calculations to experimental verifications. Nano Energy, 2017, 41, 308-319.	16.0	41
32	A novel power generation system based on the cascade utilization of coal: concept and preliminary experimental results. Energy Sources, Part A: Recovery, Utilization and Environmental Effects, 2017, 39, 1955-1962.	2.3	2
33	Carbon membrane performance on hydrogen separation in H2H2O HI gaseous mixture system in the sulfur-iodine thermochemical cycle. International Journal of Hydrogen Energy, 2017, 42, 3708-3715.	7.1	12
34	Enhanced mechanism of the photo-thermochemical cycle based on effective Fe-doping TiO2 films and DFT calculations. Applied Catalysis B: Environmental, 2017, 204, 324-334.	20.2	75
35	Study on CuO-CeO <sub>2</sub> /SiC catalysts in the sulfur-iodine cycle for hydrogen production. International Journal of Energy Research, 2016, 40, 1062-1072.	4.5	8
36	Catalytic performance and durability of Ni/AC for HI decomposition in sulfur–iodine thermochemical cycle for hydrogen production. Energy Conversion and Management, 2016, 117, 520-527.	9.2	19

#	Article	IF	CITATIONS
37	Effect of raw material sources on activated carbon catalytic activity for HI decomposition in the sulfur-iodine thermochemical cycle for hydrogen production. International Journal of Hydrogen Energy, 2016, 41, 7854-7860.	7.1	21
38	Splitting of CO <sub>2</sub> via the Heterogeneous Oxidation of Zinc Powder in Thermochemical Cycles. Industrial & Engineering Chemistry Research, 2016, 55, 534-542.	3.7	6
39	A novel photo-thermochemical cycle of water-splitting for hydrogen production based on TiO 2â^'x /TiO 2. International Journal of Hydrogen Energy, 2016, 41, 2215-2221.	7.1	33
40	Catalytic decomposition of sulfuric acid over CuO/CeO2 in the sulfur–iodine cycle for hydrogen production. International Journal of Hydrogen Energy, 2015, 40, 2099-2106.	7.1	23
41	HI Decomposition over Carbon-Based and Ni-Impregnated Catalysts of the Sulfur–Iodine Cycle for Hydrogen Production. Industrial & Engineering Chemistry Research, 2015, 54, 1498-1504.	3.7	13
42	Chromium Copper Catalysts for LiClO <sub>4</sub> Decomposition. Propellants, Explosives, Pyrotechnics, 2015, 40, 531-538.	1.6	0
43	A novel photo-thermochemical cycle for the dissociation of CO 2 using solar energy. Applied Energy, 2015, 156, 223-229.	10.1	49
44	Influence of the hydrothermal dewatering on the combustion characteristics of Chinese low-rank coals. Applied Thermal Engineering, 2015, 90, 174-181.	6.0	86
45	Thermal efficiency evaluation of a ZnSI thermochemical cycle for CO2 conversion and H2 production – Complete system. International Journal of Hydrogen Energy, 2015, 40, 6004-6012.	7.1	15
46	Catalytic performance of different carbon materials for hydrogen production in sulfur–iodine thermochemical cycle. Applied Catalysis B: Environmental, 2015, 166-167, 413-422.	20.2	25
47	Metal Oxides as Catalysts for Boron Oxidation. Journal of Propulsion and Power, 2014, 30, 47-53.	2.2	45
48	Equilibrium potential for the electrochemical Bunsen reaction in the sulfur–iodine cycle. International Journal of Hydrogen Energy, 2014, 39, 18727-18733.	7.1	8
49	Electrolysis of the Bunsen Reaction and Properties of the Membrane in the Sulfur–lodine Thermochemical Cycle. Industrial & Engineering Chemistry Research, 2014, 53, 13581-13588.	3.7	22
50	Performance of the Electrochemical Bunsen Reaction Using Two Different Proton Exchange Membranes in the Sulfur–lodine Cycle. Industrial & Engineering Chemistry Research, 2014, 53, 4966-4974.	3.7	12
51	Detailed kinetic modeling of homogeneous H2SO4 decomposition in the sulfur–iodine cycle for hydrogen production. Applied Energy, 2014, 130, 396-402.	10.1	31
52	Electrochemical characterization of electrodes in the electrochemical Bunsen reaction of the sulfur–iodine cycle. International Journal of Hydrogen Energy, 2014, 39, 7216-7224.	7.1	16
53	Effects of microwave irradiation treatment on physicochemical characteristics of Chinese low-rank coals. Energy Conversion and Management, 2013, 71, 84-91.	9.2	189
54	Electrochemical investigation of the Bunsen reaction in the sulfur–iodine cycle. International Journal of Hydrogen Energy, 2013, 38, 14391-14401.	7.1	25

#	Article	IF	CITATIONS
55	A novel thermochemical cycle for the dissociation of CO2 and H2O using sustainable energy sources. Applied Energy, 2013, 108, 1-7.	10.1	33
56	Effect of preparation method on platinum–ceria catalysts for hydrogen iodide decomposition in sulfur–iodine cycle. International Journal of Hydrogen Energy, 2008, 33, 602-607.	7.1	47
57	Hydrogen iodide decomposition over nickel–ceria catalysts for hydrogen production in the sulfur–iodine cycle. International Journal of Hydrogen Energy, 2008, 33, 5477-5483.	7.1	28
58	Catalytic Thermal Decomposition of Hydrogen Iodide in Sulfurâ^'Iodine Cycle for Hydrogen Production. Energy & Fuels, 2008, 22, 1227-1232.	5.1	27